Supplementary Information - Single Vesicle Assaying of SNARE-Synaptotagmin Driven Fusion Reveals Fast and Slow Modes of Both Docking and Fusion and Intra-Sample Heterogeneity

Sune M. Christensen, Michael W. Mortensen and Dimitrios G. Stamou

Contents

1 Crosstalk correction of fluorescence data

Experiments were conducted to quantify *(i)* crosstalk from donor (2 % DiO) labeled vesicles into the acceptor channel relative to the signal recorded in the donor channel upon excitation at 458 nm and *(ii)* cross excitation of acceptor (2 % DiI) labeled vesicles by the 458 laser line relative to direct excitation of the acceptor at 543 nm. The crosstalk evaluation was used to correct the fusion data and a control sample of premixed vesicles, which was prepared in order to simulate the product of a full fusion event and extract the corresponding single vesicle apparent FRET efficiency.

Data were recorded by confocal microscopy of single surface immobilized vesicles. The lipid composition of the vesicles was (POPC/DOPE-Biot./DiO-C_{18} 97.9:0.1:2), (POPC/ DOPE-Biot./DiI-C_{18} 97.9:0.1:2) and (POPC/DOPE-Biot./DiO-C_{18}/DiI-C_{18} 97.9:0.1:1:1). Background corrected single vesicle intensities were extracted from the micrographs. The crosstalk from DiO observed in the acceptor channel was calculated by evaluating the ratio of the signal in the acceptor channel relative to the observed signal in the donor channel, which yielded a peak value of 4 %, Fig. 1a. Similarly, the cross excitation of DiI with the 458 nm laser line relative to direct excitation was calculated to be 0.2 %, Fig. 1b. The parameters extracted from the crosstalk analysis was used to correct the measured intensities and thereby evaluate the crosstalk corrected apparent FRET efficiency ($E = I_{acc}/(I_{acc} + I_{don})$) of a premixed sample containing a 1:1 mixture of DiO and DiI, Fig. 1c.

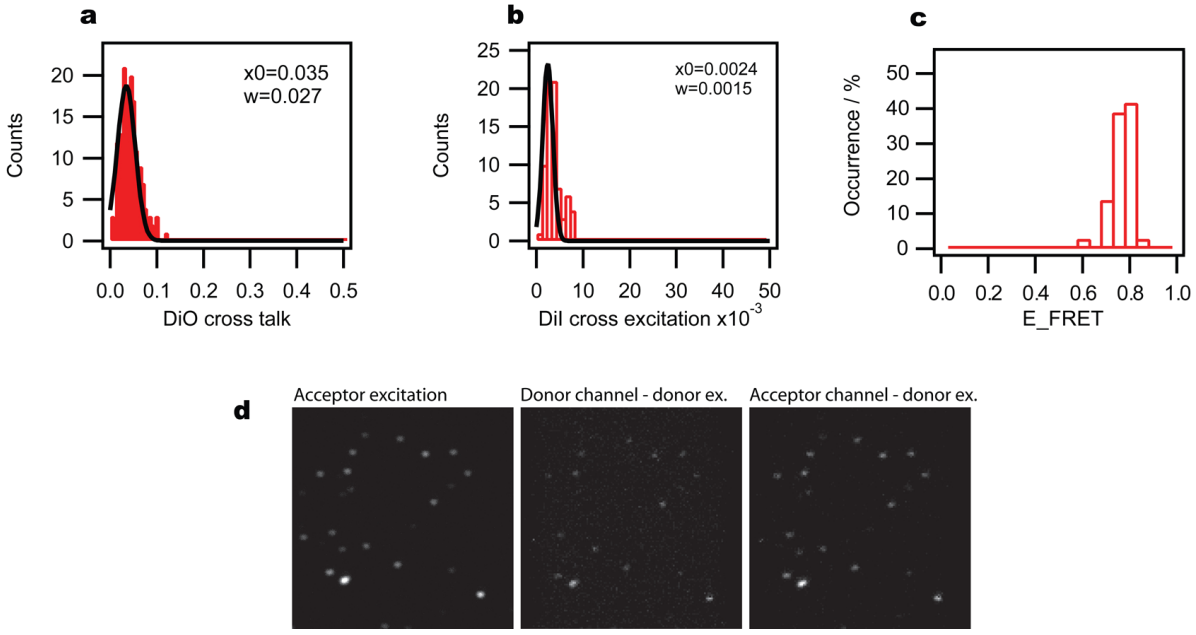

Figure 1: **Crosstalk correction of fluorescence data.** **(a)** crosstalk of the 2 % DiO sample observed in the acceptor channel relative to the signal in the donor channel. Data were fitted with a gaussian distribution. **(b)** Cross excitation relative to direct excitation of the 2 % DiI sample. **(c)** Histogram of apparent FRET efficiencies of vesicles premixed with 1 % donor and acceptor fluorophores. **(d)** Micrographs of vesicles with 1:1 donor to acceptor ratio.

2 Measuring the docking attempt frequency of diffusing v-vesicles onto stationary t-vesicles

This section provides a detailed description of the procedure applied to measure the docking attempt frequency of the diffusing v-vesicles onto the surface-immobilized t-vesicles.

The first step in the procedure was to partition the field of view of the fusion movie into an array of regions of interest (ROIs) and integrate the intensity of the v-vesicle label throughout the movie(s) inside such ROIs. Fig. 2a shows a micrograph of diffusing v-vesicles with overlaid ROIs. Definition of ROIs and integration of v-vesicle fluorescence was conducted by a script written in Igor Pro ver. 5.01.

Fig. 2c-d shows two sample ROI traces. v-vesicles diffusing into the ROIs are observed as distinct intensity spikes. We counted the v-vesicles using a threshold (dashed lines). The threshold was set automatically for each sample by demanding a confidence of 0.01 % in discriminating a diffusing v-vesicle from the background noise (i.e., statistically one false count will be detected in a given ROI in 10,000 frames). To determine the threshold that fulfill this criterion we collected the background noise recorded in all ROIs before addition of v-vesicles to the chamber, Fig. 2b, and by iterating through these data we evaluated the fraction of noise situated above a given intensity value and constructed a curve of uncertainty in v-vesicle detection vs. applied threshold, Fig. 2b inset. The threshold corresponding to 0.01 % uncertainty was read from this curve. For ROIs overlapping with immobilized t-vesicles the script filtered docking events from the counting of diffusing v-vesicles.

Using the obtained threshold a curve of the accumulated number of v-vesicles detected in the ROIs vs. time was constructed, Fig. 2e, and fitted with a straight line to extract the count frequency. In the given example 207.58 ± 0.03 vesicles were detected in all ROIs per sec. (this experiment had 676 ROIs in total). With a time resolution of 0.202 s this amounts to 42 vesicles per frame.

With the average count of vesicles inside the ROIs determined the concentration is obtained as

$$C = \frac{N_{avg} K}{N_{ROIs} V_{ROI}} \tag{1}$$

where N_{avg} denotes the average vesicle count per frame, N_{ROIs} the total number of ROIs and V_{ROI} the volume of a single ROI cube. K is a correction factor that becomes necessary due to the limited speed of confocal laser scanning, for which reason only a fraction of the v-vesicles can be counted with this apporach. V_{ROI} and K are discussed further below.

2.1 Correction of *in situ* determined vesicle concentrations for underestimation due to diffusion

Due to diffusion and the limited time resolution of confocal raster scanning the v-vesicle concentration obtained by counting the number of diffusing particles is systematically underestimated by the ROI approach. As an example, a vesicle initially present at the bottom of a ROI when the first line is scanned might have left the ROI before the last line of the ROI is scanned and in this way escape detection. To account for this artifact we devised a correction procedure.

The procedure is based on the fundamental assumption that a diffusing vesicle gives enough signal to be detected *only* if it remains within the x and y boundaries of a ROI and within a height from the surface corresponding to at least 50 % detection efficiency during the time it takes to sample it by confocal raster scanning (this assumption was verified by the successful measurement of the concentration of a calibration sample, see below). Based on this assumption, the z dimension of the ROIs used for object counting was found to $L_z = 457$ nm by inspection of the point-spread-function of the microscope measured upon reflection of the laser at the glass

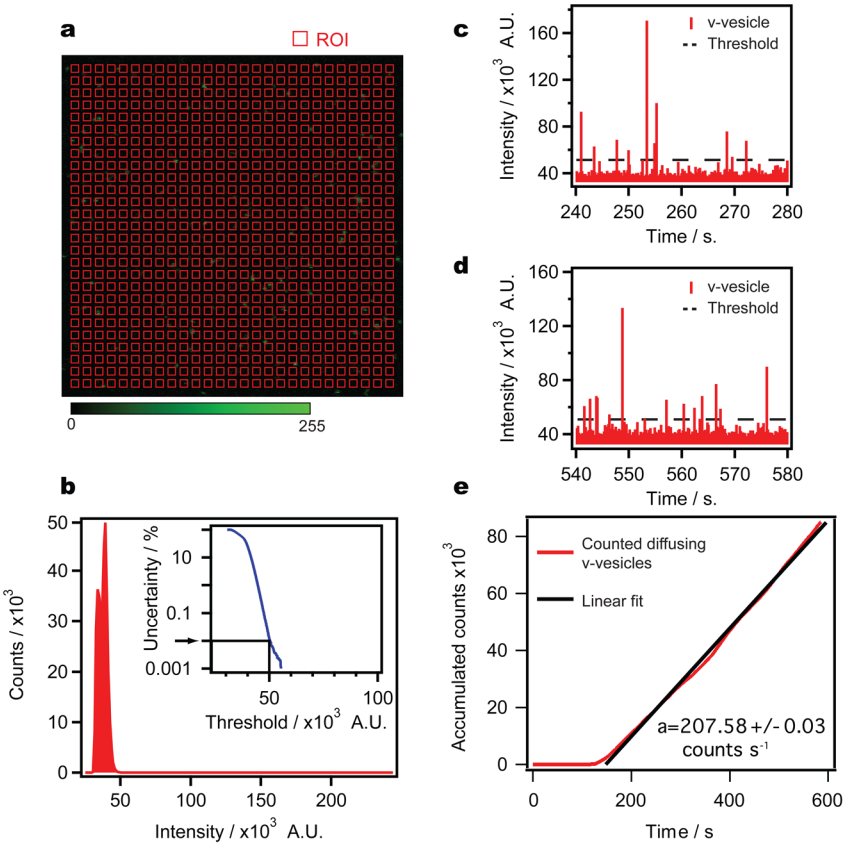

Figure 2: **ROI based approach for counting diffusing vesicles.** **(a)** A snapshot from the fusion movie showing diffusing v-vesicles with overlaid ROIs used for integrating the fluorescence signal and thereby count the number of diffusing particles. **(b)** Histogram of the background noise measured before addition of v-vesicles to the chamber. The noise histogram was used for calculating the confidence in discriminating v-vesicles from background with a given intensity threshold (inset). The threshold was assigned systematically for each sample by demanding a confidence of 0.01 %. **(c-d)** Sample ROI traces of diffusing v-vesicles (spikes). The threshold used for counting the vesicles is indicated by the dashed lines. **(e)** Accumulated count of diffusing vesicles observed in 676 ROIs during an experiment. A linear fit of the data revealed the average v-vesicle count (a=207.58 $\pm$ 0.03 counts s^{-1}). In this case the time resolution was 0.202 s/frame and thus an average of 42 v-vesicles were counted in the 676 ROIs per frame.

interface (Fig. 3a). In the experiments concerned here the size of one pixel was 50x50 nm^2 and the x and y dimension of the ROI was 10 pixels. With the applied experimental settings the time to scan a 10x10 pixel ROI was $t_{ROI} = 7.14$ ms. A sketch of the ROI cube along with definition of axes is given in Fig. 3b.

We now estimate the fraction of vesicles that are too fast to be captured by the ROI approach. The diffusion coefficient of the vesicles can be deduced from the Stokes-Einstein relation:

$$D = \frac{k_B T}{6\pi\eta r} \tag{2}$$

Where k_B is the Boltzmann factor, T is temperature, η denotes the viscosity of the medium and r the vesicle radius. The time evolution of the probability density to find a particle at position x if started at $x = 0$ is given by Einsteins diffusion equation [Einstein, A. Über die von der molekularkinetischen Theorie der Wärme geforderte Bewegung von in ruhenden Flüssigkeiten suspendierten Teilchen. Annalen der Physik 1905, 17, 549.]:

$$\rho(x,t) = \frac{1}{\sqrt{4\pi Dt}} e^{\frac{-x^2}{4Dt}} \quad , \quad \int_{-\infty}^{\infty} \rho(x,t)dx = 1 \tag{3}$$

The probability, $P_{in}(x)$, that a vesicle will remain within a ROI of length L if started at position x with respect to the ROI center is now evaluated. Since brownian motion in orthogonal directions is independent, the problem can be solved in one dimension and then extrapolated to include all three dimensions. $P_{in}(x)$ is obtained as:

$$P_{in}(x) = \int_{-x-\frac{L}{2}}^{-x+\frac{L}{2}} \rho(x)dx \quad , \quad x \in]-\frac{L}{2}, \frac{L}{2}[\tag{4}$$

$$P_{in}(x) = \frac{1}{2}\left[erf(\frac{-x+\frac{L}{2}}{\sqrt{4Dt}}) - erf(\frac{-x-\frac{L}{2}}{\sqrt{4Dt}})\right] \tag{5}$$

Where $erf(x) = \frac{2}{\sqrt{\pi}} \int_0^x e^{-u^2} du$. The average probability for a vesicle to remain within the ROI, if present at a random coordinate at $t = 0$, is obtained by averaging:

$$\langle P_{in}(x) \rangle = \frac{1}{L} \int_{-L/2}^{L/2} P_{in}(x)dx \Rightarrow \tag{6}$$

$$\langle P_{in}(x) \rangle = erf(K) + \frac{e^{-K^2} - 1}{\sqrt{\pi} K} \quad , \quad K = \frac{L}{\sqrt{4Dt}} \tag{7}$$

In the z-direction (normal to the surface) vesicles can only leave the ROI at the off surface side. To take this into account $P_{in}(z)$ was evaluated treating the surface as an absorptive wall[1], the only difference to $P_{in}(x)$ being that one of the integration borders is substituted for infinity. The result is:

$$\langle P_{in}(z) \rangle = \frac{1}{2}\left(1 + erf(K_z) + \frac{e^{-K_z^2} - 1}{\sqrt{\pi} K_z}\right) \quad , \quad K_z = \frac{L_z}{\sqrt{4Dt}} \tag{8}$$

Finally, the resulting probability that a vesicle situated within the ROI at time zero will remain there within the ROI scanning time is given by:

$$P_{in} = \langle P_{in}(x) \rangle \langle P_{in}(y) \rangle \langle P_{in}(z) \rangle \tag{9}$$

$$P_{in} = \frac{1}{2}\left(erf(K) + \frac{e^{-K^2} - 1}{\sqrt{\pi} K}\right)^2 \left(1 + erf(K_z) + \frac{e^{-K_z^2} - 1}{\sqrt{\pi} K_z}\right) \tag{10}$$

To extract the correction factor we finally considered the size distribution of the v-vesicles, Fig. 4a. This was accomplished by inserting $D(r)$ according to the Stokes-Eintein relation in Eq. 10 resulting in a curve of the detectable fraction of vesicles as a function of size, Fig. 4b. The percentage of detectable vesicles in the experiments was obtained by combining the curves of P_{in} and the v-vesicle size distribution yielding a detectable fraction of 22.29 % of the vesicles. The correction factor for the vesicle count thus becomes $K = 4.5$.

For the concentration of v-vesicles in the experiment in Fig. 2 we thus obtain:

[1] in other words, a vesicle that hits the surface is considered to remain within the ROI in t_{ROI}

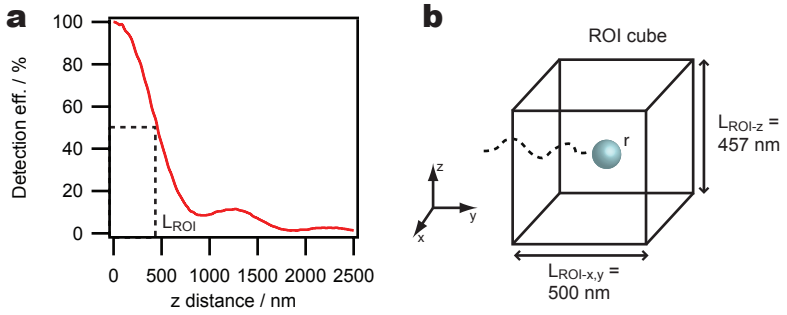

Figure 3: **Dimensions of ROI cube used for concentration measurements. (a)** Normalized point spread function. The dimensions of the cubic ROI is fixed as the distance from the surface where the intensity reaches 50 % of the value at z=0. **(b)** Sketch of the ROI cube with dimensions as used in the reported experiments.

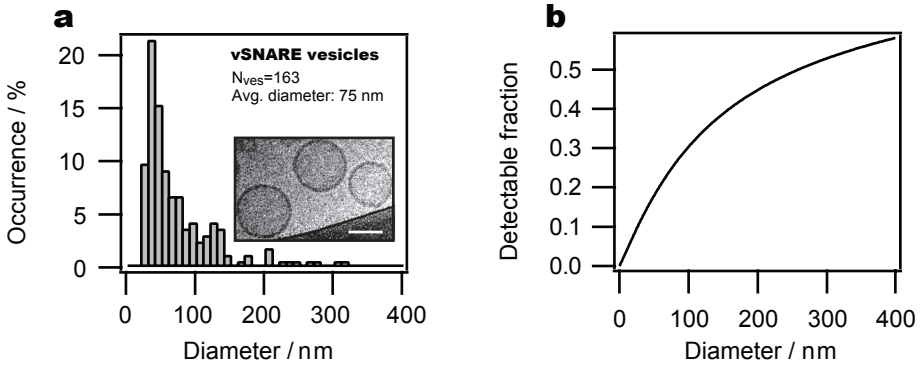

Figure 4: **Detectable fraction of vesicles as a function of size. (a)** Size distribution as measured by cryoTEM. **(b)** Percentage of vesicle that statistically can be detected with the given experimental setup.

$$C = \frac{N_{avg}K}{N_{ROIs}V_{ROI}} \quad \Rightarrow \tag{11}$$

$$C = \frac{42 \text{ vesicles x } 4.5}{676 \text{ x } 500 \text{ x } 500 \text{ x } 457 \text{ nm}^3} = 2.45 \text{ x } 10^{-9} \text{ vesicles/nm}^3 \quad \Rightarrow \tag{12}$$

$$C = 4.07 \text{ nM} \tag{13}$$

To verify the described method we applied it to measure the concentration of a sample of fluorescently labeled beads (Fluorospheres, Molecular Probes, catalog number F8766) with a known concentration. The beads had a nominal radius of 18 nm and are thus comparable in dimensions to the v-vesicles. The concentration of the beads ([C]=0.30 nM) was measured successfully on two independent samples and each measurement fell within 10 % deviation of the expected value ([$C_{measured-1}$]=0.28 nM and [$C_{measured-2}$]=0.32 nM). Fig. 5 provides the counting data for the beads along with the experimental parameters.

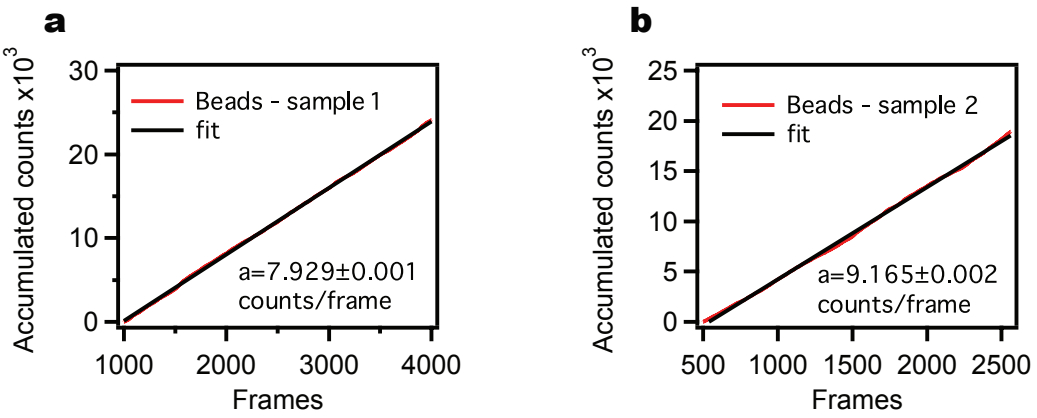

Figure 5: **Method verification: fluorescently labeled beads with a concentration of 0.30 nM. (a-b)** Accumulated count of detected beads in all ROIs measured on two independent samples. 144 ROIs were applied for each sample. In these experiments we had V_{ROI}= 8.71 x 10^{-19} m^3 and K=2.66 yielding a concentration of 0.28 nM for the data in (a) and 0.32 nM for the data in (b).

2.2 Obtaining the docking attempt frequency from the v-vesicle concentration

The diffusion current, I (hits s^{-1}), of a solute onto a spherical particle in a solution is a standard result of diffusion theory (see Berg, H.C. (1993). Random Walks in Biology (Princeton University Press)):

$$I = 4\pi DrC \tag{14}$$

In our case D is the diffusion coefficient of the v-vesicles, r the radius of the t-vesicle and C the v-vesicle concentration. To take into account that v-vesicles can approach only from the off surface side we multiplied Eq. 14 by a factor of 0.5. Furthermore, the v-vesicles have dimensions comparable to the binding targets which we took into account by setting $r = r_v + r_t$ where r_v and r_t denote the average radii of the respective vesicles:

$$I = 2\pi D(r_v + r_t)C \tag{15}$$

D was calculated as 5.71 $\mu m^2/s$ using the Stokes-Einstein equation ($D = kBT/6\pi hr$) with T=293.15 K, a viscosity (h) of 1.002 x 10^{-3} Pa s and applying the average v-vesicle radius from the cryoTEM data (r_v=37.5 nm). For calculating I we againg used the average vesicle radii from the cryoTEM data (r_t=26 nm). Using Eq. 15 we obtained an (average) docking attempt frequency of 5.62 hits/s for the experiment shown in Fig. 2.

3 Maximum-likelihood fitting for determination of docking probabilities

This section describes in more detail the method used for extracting the intrinsic docking probability, p_d, upon collision of a diffusing v- and an immobilized t-vesicle from measured lists of number of attempts before successful docking. The basis of this approach is the assumption that docking is a stochastic event. The problem is simplified by assuming that one distinct binding mode dominates the docking process for each configuration of proteins and or Ca^{2+}. Our data sets consist of observations of number of attempts to successful docking and observations of t-vesicles that did not bind within experimental time after having experienced a given number of attempts. In the first case, the probability to observe binding after n_a attempts is given by the product of the probability to observe one successful attempt, p_d, preceded by $n_a - 1$ unsuccessful attempts (the geometrical distribution):

$$P_{docking}(n_a) = p_d(1-p_d)^{n_a-1} \tag{16}$$

Conversely, the probability to observe a t-vesicle that did not bind a v-vesicle after n_a attempts is given by:

$$P_{no\ docking}(n_a) = (1-p_d)^{n_a} \tag{17}$$

The joint probability to observe a given data set is then given by the product of the individual probabilities:

$$P_J = \prod_{i=1}^{N} P_{docking,i}(n_{a,i}) \prod_{i=1}^{N'} P_{no\ docking,i}(n_{a,i}) = \prod_{i=1}^{N} p_d(1-p_d)^{n_{a,i}-1} \prod_{i=1}^{N'} (1-p_d)^{n_{a,i}} \tag{18}$$

According to the method of maximum-likelihood the best estimation of the free parameter p_d is the one that maximizes the joint probability of the data. To determine the maximum of the joint probability P_J was calculated by iterating through the possible values of p_d (here, 10,000 iterations were performed).

To evaluate the capability of the method for obtaining p_d we simulated data using a random number generator (*enoise* function in IgorPro ver. 5.01). The random number generator delivered a number, k, between 0 and 1, which was used as a representative of a docking attempt. An attempt was then categorized as successful if $k < p_d$. If $k > p_d$ iterations were continued up to a defined maximum number of attempts/trials (simulating the observation time in the experiments). In this manner lists of attempts before docking and lists of failed attempts for vesicles that did not exhibit docking within the maximun number of trials were generated. We performed the simulations with a fixed number of 100 binding targets, which is comparable to the number of t-vesicles in the experiments. Figure 6a shows an example of the accumulated number of docking events after n_a attempts for a simulation with p_d =0.01 and allowing a maximum of 1000 trials for each docking target (in this case all docking targets bound within the observation time). The lists of attempts to docking and attempts without docking were then used as input in the calculation of the joint probability (Eq. 18) which we maximized to extract p_d. The standard deviation, σ, was extracted by normalizing P_J and fitting it with the normal distribution, $G(x, \sigma)$, according to:

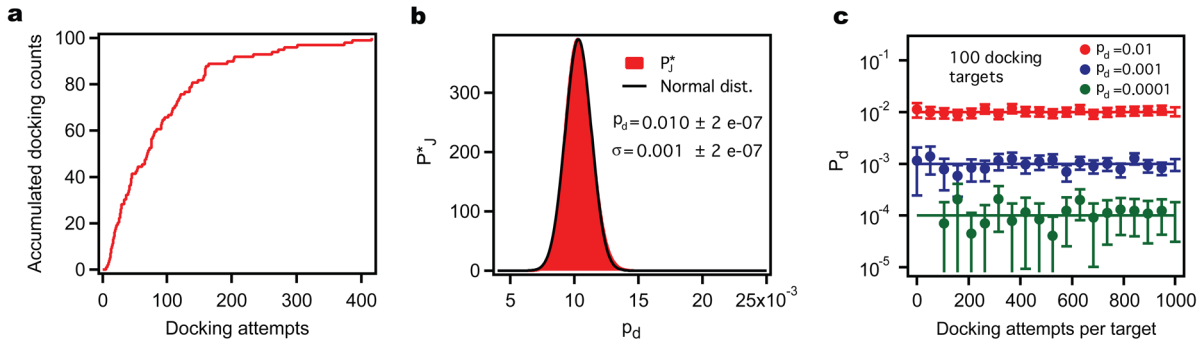

Figure 6: **Method of maximum-likelihood for measuring docking probabilities. (a)** Simulated dataset of the accumulated number of attempts before successful docking for N =100 docking targets. **(b)** Normalized joint probability (P_J^*) calculated for the dataset in a and fitted with the normal distribution to obtain the peak location, P_d, and the standard deviation, σ. **(c)** p_d obtained from simulated datasets with N =100 docking targets and three different input values of p_d as a function of the number of observed docking attempts (the number of observed docking attempts depends on the concentration of diffusing vesicles and the time of observation in a given experiment.

$$P_J^* = \frac{P_J}{\int_0^1 P_J(p_d)dp_d} \tag{19}$$

$$G(x,\sigma) = \frac{1}{\sigma\sqrt{2\pi}} e^{\frac{-(x-x_0)^2}{2\sigma^2}} \tag{20}$$

Figure 6b shows P_J^* for the dataset in figure 6a . As expected, the joint probability peaks at the input value of $p_d = 0.01$. The standard deviation was on the order of 10%. To further characterize the method p_d was obtained from simulated datasets with $p_d = 10^{-2}$,$p_d = 10^{-3}$ and $p_d = 10^{-4}$ as a function of the maximum number of trials (experimentally, the maximum number of trials is defined by the concentration of diffusing v-vesicles and the time of observation in a given experiment.)

4 Size distributions of vesicles prepared by direct reconstitution

Vesicle radius was quantified using a technique recently developed in our lab (Kunding *et al.*, Biophysical J., Vol 95, p. 1176, 2008 and Lohr *et al.*, Meth. Enzymoogy, Vol. 465, p. 143-160. 2009) to calibrate the fluorescence intensity of single immobilized vesicles into physical size. The size-calibration was performed by examining a vesicle sample extruded 10 times through 50 nm filters using both dynamic light scattering (DLS) and confocal fluorescence microscopy

Dynamic light scattering was performed using an ALV-5000 Correlator equipped with a 633 nm laser. Vesicles were diluted to a final concentration of 0.01% (w/v) in 0.02 μm filtered buffer. The size distribution was measured at 90° and the scattered intensity was collected for 10 x 30 s. To ensure that the evaluated peaks were related to translational diffusion, angle-dependent measurements were conducted at 70° , 90°, 110°, and 130° and the scattered intensity was measured for 3 x 10 s at each angle. Data were collected at 20 °C. The correlation function was translated into the number weighted size distribution using the dls 2g(t) regularized fit routine implemented in the ALV correlator software. The form factor of vesicles with a membrane thickness of 4.5 nm was applied to all data.

The background corrected integrated intensities of the vesicles were collected from the micrographs by fitting each diffraction limited spot with a two-dimensional Gaussian bell and evaluating the volume. A distribution of intensities was constructed. and the intensity distribution obtained by fluorescence was then calibrated using the DLS data according to the relation:

$$d = A\sqrt{I} \tag{21}$$

Where d is the vesicle diameter, A a proportionality factor and I the measured integrated intensity of a vesicle. A was calculated by inserting the mean radius of the population as measured by DLS (35 nm) and the mean intensity value as measured by fluorescence microscopy in Eq. 21. Once A is known the size of any vesicle labeled with the calibrated fluorophore can be obtained from the measured intensity. Two vesicle samples were prepared to calibrate the intensity to size conversion for respectively donor and acceptor labeled vesicles. Figure 7 shows size distributions obtained by the described procedure of v- and t-vesicles prepared by the direct reconstitution method.

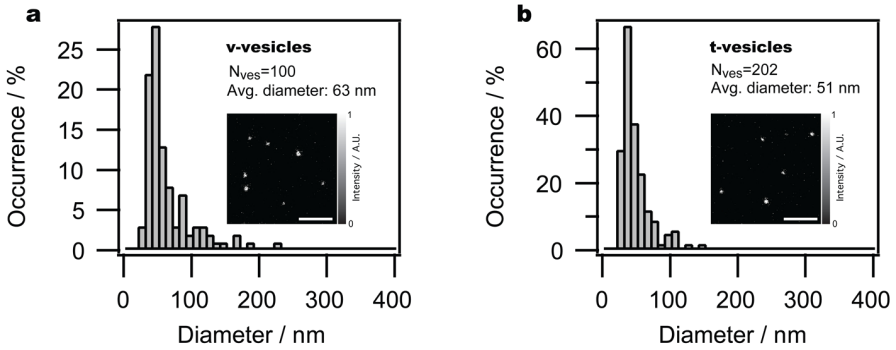

Figure 7: **Size distribution of SNARE vesicles prepared by the direct reconstitution method.** Bars: 5 μm.

5 Additional events from the lipid mixing analysis

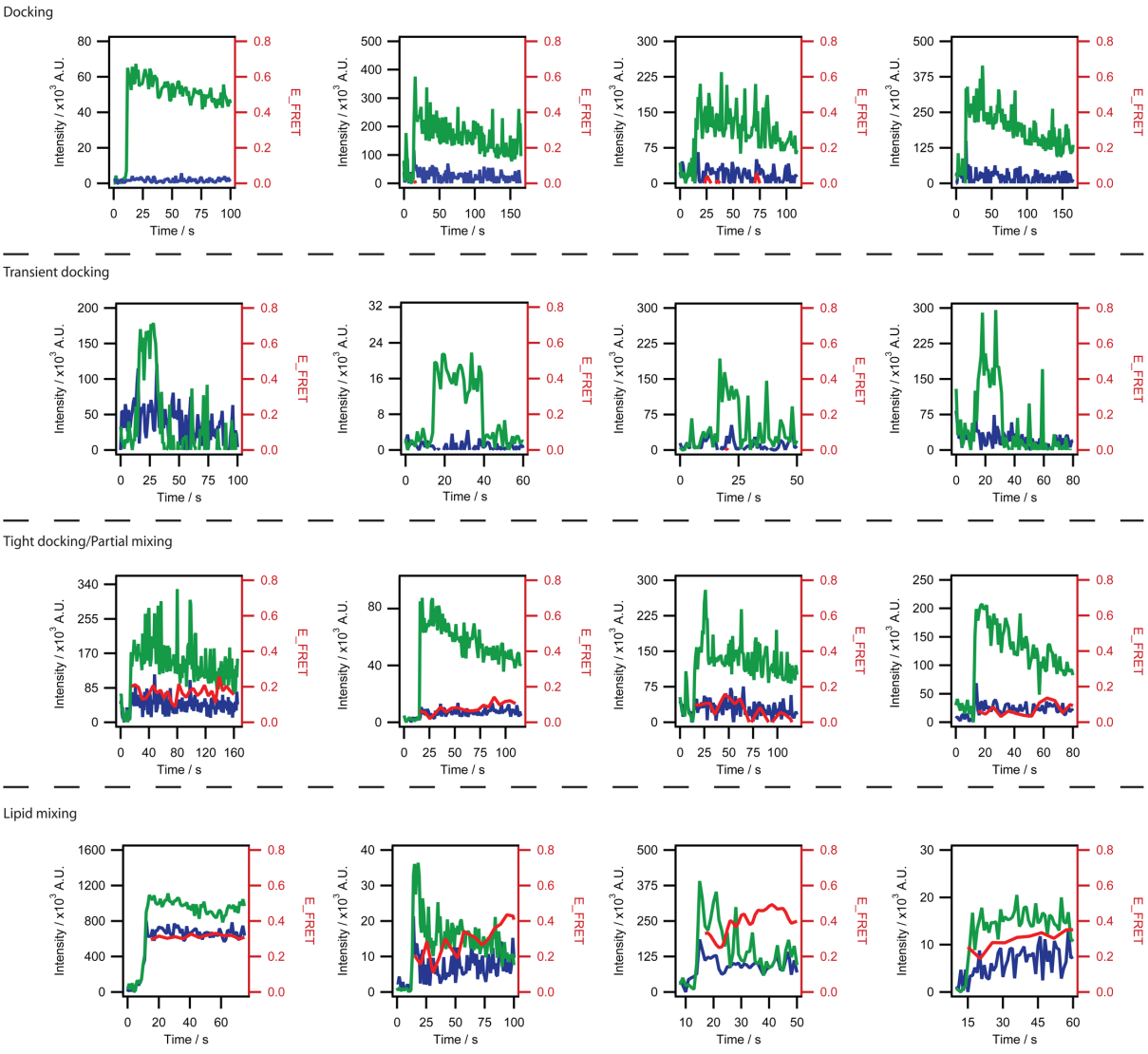

Figure 8: **Additional event examples.** Green: donor, blue: acceptor and red: E_FRET.